Author Manuscript

Author Manuscript

Author Manuscript

Author Manuscript

HHS Public Access

Author manuscript

Biosens Bioelectron. Author manuscript; available in PMC 2017 March 15.

Published in final edited form as:

Biosens Bioelectron. 2016 March 15; 77: 188–193. doi:10.1016/j.bios.2015.09.017.

3D-Printed Supercapacitor-Powered Electrochemiluminescent Protein Immunoarray

Karteek Kadimisetty[a,1], **Islam M. Mosa**[a,b,1], **Spundana Malla**[a], **Jennifer E. Satterwhite-Warden**[a], **Tyler Kuhns**[a], **Ronaldo C. Faria**[c], **Norman H. Lee**[d], and **James F. Rusling**[a,e,f,g,*]

[a]Department of Chemistry, University of Connecticut, Storrs, CT 06269, USA [b]Department of Chemistry, Tanta University, Tanta, 31527, Egypt [c]Departamento de Química, Universidade Federal de São Carlos, São Carlos, SP, Brazil [d]Department of Pharmacology & Physiology, George Washington Univ., Washington, DC, USA [e]Department of Cell Biology, University of Connecticut Health Center, Farmington, CT 06032 [f]School of Chemistry, National University of Ireland at Galway, Ireland [g]Institute of Materials Science, University of Connecticut, Storrs, Connecticut 06269, United States

Abstract

Herein we report a low cost, sensitive, supercapacitor-powered electrochemiluminescent (ECL) protein immunoarray fabricated by an inexpensive 3-dimensional (3D) printer. The immunosensor detects three cancer biomarker proteins in serum within 35 min. The 3D-printed device employs hand screen printed carbon sensors with gravity flow for sample/reagent delivery and washing. Prostate cancer biomarker proteins, prostate specific antigen (PSA), prostate specific membrane antigen (PSMA) and platelet factor-4 (PF-4) in serum were captured on the antibody-coated carbon sensors followed by delivery of detection-antibody-coated $Ru(bpy)_3^{2+}$ (RuBPY)-doped silica nanoparticles in a sandwich immunoassay. ECL light was initiated from RuBPY in the silica nanoparticles by electrochemical oxidation with tripropylamine (TPrA) co-reactant using supercapacitor power and ECL was captured with a CCD camera. The supercapacitor was rapidly photo-recharged between assays using an inexpensive solar cell. Detection limits were 300–500 fg mL^{-1} for the 3 proteins in undiluted calf serum. Assays of 6 prostate cancer patient serum samples gave good correlation with conventional single protein ELISAs. This technology could provide sensitive onsite cancer diagnostic tests in resource-limited settings with the need for only moderate-level training.

*Correspondence should be addressed to J.F.R. (james.rusling@uconn.edu).

[1]These authors contributed equally to this work.

Publisher's Disclaimer: This is a PDF file of an unedited manuscript that has been accepted for publication. As a service to our customers we are providing this early version of the manuscript. The manuscript will undergo copyediting, typesetting, and review of the resulting proof before it is published in its final citable form. Please note that during the production process errors may be discovered which could affect the content, and all legal disclaimers that apply to the journal pertain.

Supplementary Information Supplementary data associated with this article can be found in the online version

Schematic representation of screen printing carbon electrodes and immunosensor chip assembly. Synthesis and characterization of RuBPY-Si nanoparticles, chemistry of ECL detection, and electrochemical characterization of carbon electrodes. Electroanalytical characterization of supercapacitor. Optimization of detection antibody conditions, single biomarker detection; correlation data for patient samples. A link for CAD files.

The authors declare no competing financial interest.

Author Manuscript Author Manuscript Author Manuscript Author Manuscript

Keywords

3D-printing; ECL immunoarray; microfluidics; supercapacitor; biomarker proteins; Prostate Cancer

1. Introduction

The recent emergence of inexpensive 3D printers offers revolutionary low cost options for designing and constructing biosensor systems (Gross, B.C., et al., 2014). Fabrication of microfluidic devices by 3D-printing has been explored for rapid prototyping. Early applications include master for faster production of microfluidic channels from poly(dimethylsiloxane) (PDMS) (McDonald et al., 2002) and reaction ware for chemical synthesis and spectroscopic analysis (Symes et al., 2012; Dragone et al., 2013). Flow injection systems for monitoring metal ions (Su et al., 2014), add-on accessories for turning smartphones into sensors for food allergens and albumin have been printed (Coskun & Wang, et al., 2013; Wei et al., 2014; Coskun & Nagi, et. al, 2013; Roda et al., 2014; Wei et al., 2014). Milli- and microfluidic devices have been printed for nanoparticle synthesis (Femmer et al., 2014; Kitson et al., 2012). Other applications include calorimetry (Shallan et al., 2014), cell growth monitoring (Anderson et al., 2013), blood evaluation (Chen et al., 2014) and pathogenic bacteria detection (Lee et al., 2015). Electrochemical sensing integrated into a 3D-printed fluidic device was used to detect dopamine and nitric oxide (Erkal et al., 2014). We recently reported a 3D-printed microfluidic amperometric sensor for hydrogen peroxide (Bishop et al., 2015).

Microfluidic arrays integrating complex procedures into simple, portable, inexpensive diagnostic platforms will be valuable for future personalized healthcare (Yager et al., 2006; Rusling, 2013). Detection of biomarker panels holds great promise for early cancer detection and monitoring (Hawkridge et al., 2009; Wulfkuhle et al., 2003; Kingsmore, 2006; Giljohann et al., 2009; Rusling et al., 2010), promises improved therapeutic outcomes (Siegel et al., 2014). Ideally, widespread clinical applications will require low cost, low tech, multiplexed assay devices (Hawkridge et al., 2009; Wulfkuhle et al., 2003; Kingsmore, 2006; Giljohann et al., 2009; Rusling et al., 2010, Rusling, 2013). Sensitive, fast, accurate multiplexed protein detection has been achieved using conventionally fabricated microfluidic arrays integrated with nanoscale materials (Kingsmore, 2006; Giljohann et al., 2009; Rusling et al., 2010; Rusling et al., 2014).

Microfluidic array devices are often made using lithography, injection molding (Weibel et al., 2005; Urbanski et al., 2006; Hulme et al., 2009; Sudarsan et al., 2006; Chin et al., 2011; Laksanasopin et al., 2015), but prototype development time and cost can be limiting factors. Both approaches require economies of scale to become cost effective. We have developed microfluidic arrays for multiple biomarker detection using molded or precision cut microfluidic channels. We coupled amperometric detection on gold nanostructured sensor arrays with magnetic particles massively loaded with enzyme labels and antibodies, and demonstrated simultaneous ultrasensitive detection of up to four cancer biomarker proteins (Chikkaveeraiah et al., 2011; Malhotra et al., 2012; Otieno et al., 2014). We also developed

Author Manuscript Author Manuscript Author Manuscript Author Manuscript

electrochemiluminescent (ECL) (Forster et al., 2009) arrays with antibody-coated $Ru(bpy)_3^{2+}$ (RuBPY)-doped silica nanoparticles for detection on single wall carbon nanotube forests patterned on pyrolytic graphite chips (Sardesai et al., 2013; Kadimisetty et al., 2015). Both approaches utilized non-lithographic fabrication to achieve ultrasensitive detection of multiple proteins in short assays (~35 min). Nonetheless, decreasing time and cost of prototyping and optimizing such devices may lead to benefits in faster translation to public health care (Au et al., 2015).

Electronically simple, miniature power sources are also important for clinical immunoarray development. Small supercapacitors, i.e. high performance electrochemical capacitors (EC) that store electrical energy (Simon et al., 2014), have not been widely explored for powering sensors. They have unique advantages including high power density, multiple cycling capability (Aradilla et al., 2014) and fast charge-discharge rates (Wang et al., 2012). There are few reports of integrating supercapacitors into analytical systems for signal amplification (Wang et al., 2015; Ge et al., 2013), but no examples of powering biosensors.

Herein we report a 3D-printed, gravity flow microfluidic immunoarray for multiple protein detection. These arrays are powered by inexpensive light-rechargeable supercapacitor costing **€**10 that supplies voltage to screen-printed carbon electrodes for ECL light generation that is detected by CCD camera. Simultaneous measurement of prostate cancer biomarkers, prostate specific antigen (PSA) (Telesca et al., 2008; Lilja et al., 2008), prostate specific membrane antigen (PSMA) and platelet factor-4 (PF-4) (Chikkaveeraiah et al., 2009) was achieved at clinically relevant detection limits 0.3–0.5 pg mL^{-1}. To our knowledge, this is the first 3D-printed microfluidic immunosensor, and first application of supercapacitors to a voltage-driven biosensor. Assays of human serum from cancer patients and cancer-free controls gave good correlations to single-protein enzyme-linked immunosorbent assays (ELISA).

2. Materials and methods

2.1 Chemicals and Materials

Polylactic acid (PLA) filaments, 1.75 mm diameter for 3D-printing were from MakerBot. Carbon graphite (C2050106D7) and silver/silver chloride inks (C2051014P10) were from Gwent Electronics. Poly(diallyldimethylammoniumchloride) (PDDA), poly(acrylic acid) (PAA), bovine serum albumin (BSA), 1-(3-(Dimethylamino)propyl)-3-ethylcarbodiimidehydrochloride (EDC) and N-hydroxysulfosuccinimide (NHSS) were from Sigma. Pooled human serum samples were from Capital Biosciences and individual patient serum samples were provided by George Washington University Hospital. Calf serum as a surrogate for human serum (Malhotra et al., 2010) was used for all calibrations with standard proteins. See supplementary information (SI) file for complete experimental details.

2.2 Array Device Fabrication

A commercial desktop 3D Fused Deposition Modeling (FDM) printer, MakerBot Replicator 2×, was used. The microfluidic immunoarray was printed from polylactic acid (PLA)

Author Manuscript Author Manuscript Author Manuscript Author Manuscript

(Martin et al., 2001). Initially, a computer-aided design (CAD) was created with 123D Design (Autodesk), and converted to 3D printer format using splicing software. Optimized printer settings are heated platform was set to 60 °C and extruder temperature was 230 °C, with layer height 200 μm. Extruder speed while travelling was optimized at 80 mm s^{-1}, whereas speed while extruding was 40 mm s^{-1}.

Fig. 1A shows the main array printed with 40 mm length × 30 mm width of the base. It has three reagent chambers connected to a common downstream microfluidic channel (Fig. S1, SI). The volume of the reagent chambers is 170 ± 5 μL and the volume required for the microfluidic channel to fill completely is 160 μL. Reservoir volumes were chosen to completely fill the detection channel in a horizontal position under hydrostatic pressure. The reservoirs are prefilled with sample or reagents through port holes located in custom fit 3D-printed inserts (Fig. 1A) with rods that seal the outlets of the reservoirs. Flow of sample and reagents is controlled by placing the insert to seal the reservoir, or removing it to drain the reservoir into the detection channel in a horizontal position. All reagents are prefilled on the array, and the operator needs only to release reagents sequentially by removing the inserts.

Fig. 1B shows the add-on wash reservoir designed to work with a lever-assisted moving platform device that accommodates the sensor array, wash reservoirs and a waste collector at the bottom. The wash reservoir was designed to align with reagent reservoirs of the main array and is 68 mm length × 44 mm width × 26 mm height with capacity of ~1.6 mL buffer. Wash buffer in these reservoirs is used to wash off excess sample/reagent from the main array microfluidic channels after the immunoassay. Wash reservoirs employ custom fit inserts to turn flow on and off similar to the reagent chambers. Normal load position has the detection channel with the sensors horizontal. Changing the lever on the wash reservoir to wash position provides a 25° tilt angle to the sensor array (Fig. 1B), which enables washing of the immunoreagents to a waste chamber at the bottom of the detection channel.

The sensor electrodes were fabricated by hand screen printing carbon graphitic ink using a patterned adhesive-backed vinyl mask template (Afonso et al., 2015 in press). First, a mask template was designed using AutoCAD and converted to compatible format for cutting, then a vinyl mask was cut using a portable precision desktop cutter (Cameo®, Silhouette America, Inc.). A vinyl sheet was patterned with a common working electrode and a counter electrode. Then, this vinyl mask was transferred onto heat resistant transparency film (Highland™ 707 clear film) and screen printing was done by spreading a thin layer of carbon graphitic ink evenly over the patterned surface, followed by heating at 90 °C for 15 min. Subsequently, the adhesive vinyl mask was removed revealing the patterned screen printed electrodes (Fig. S2A). A patterned 100 μm thick lamination film with holes revealing the electrodes was also made by precision cutting. These lamination films were sealed onto the pattern of electrodes in a heat press at 110 °C, creating hydrophobic microwells around the sensors that hold up to 5 μL of aqueous solution (Fig. S2B). Lastly, a template was patterned from transparency film to print Ag/AgCl paste reference electrode (Fig. S2B). The laminated, screen-printed sensor assembly was then attached to the 3D-printed immunoarray using silicone glue (Proseal clear RTV silicone adhesive sealant), which was dried for at least 2 hr (Fig. S2C).

Author Manuscript Author Manuscript Author Manuscript Author Manuscript

Supercapacitors (Cellergy, 2.1 V, 80 mF) used to power ECL arrays were low equivalent series resistance (ESR) aqueous state electrolyte, high output electrochemical double layer capacitors (EDLC's). A solar panel (Sparkfun, 0.45 W, 94 mA) was used to charge the supercapacitor to 1.5 V under ambient room, sun, or iPhone light. Voltage was checked with a digital multimeter prior to every experiment to ensure accuracy. ECL was generated by electrochemical oxidation of both tripropylamine (TPrA) and RuBPY on the sensors when 1.5 V was applied. This initiates a complex redox pathway involving RuBPY in the silica nanoparticle and results in electronically excited $[RuBPY]^{2+*}$ that emits light at 610 nm (Miao et al., 2004; Forster et al., 2009). Generated ECL was captured from the sensor array using a CCD camera (Sardesai et al., 2013)

RuBPY-silica nanoparticles (RuBPY-SiNP) with average diameter of 117 ± 10 nm were synthesized and characterized as described previously and coated with successive layers of PDDA and PAA, followed by covalently linking secondary antibodies to –COOH groups of PAA (Fig. S3&S4, SI) (Sardesai et al., 2009). Three different RuBPY-SiNP-Ab_2 were prepared featuring anti-PSA, anti-PSMA and anti-PF-4 as Ab_2. Optimized Ab_2 concentrations for attachment onto RuBPY-SiNPs were 8 μg mL^{-1} for PSA, and 7.5 μg mL^{-1} for PSMA and PF-4 (Fig. S5, SI). For simultaneous detection of all 3 proteins, the three RuBPY-SiNPs were mixed in equal proportions. The Ab_2/RuBPY-SiNP ratio was measured at 38:1 (see SI). Estimated yield for preparation of silica nanoparticle-Ab_2 bio-conjugate is ~47 % per batch in terms of silicon reagent, and cost is €0.20 per assay. Covalent linking of antibodies to RuBPY silica nanoparticles has been successfully used previously (Sardesai et al., 2009; Kadimisetty et al., 2015) and are stable for 30 days or more when stored at 4°C. TprA at 350 mM in 0.2 M phosphate buffer + 0.05% Tween-20 (T_{20}) and 0.05% Triton-X at pH 7.5 was used as ECL co-reactant.

2.3 Assay Procedure

Carbon sensors were modified by covalently attaching capture antibody (Ab_1) using EDC-NHSS. Complete details in supplementary information. Ab_1-coated sensors were incubated with 1 % casein in PBS for 1 hr to minimize non-specific binding (NSB). These capture antibody coated carbon sensors are stable up to 7 days when stored at 4°C. Reagent chambers on the array were prefilled with serum samples, detection antibody (Ab_2)-coated RuBPY-SiNP dispersions, and TprA solution. Serum samples (2–5 μL) were first diluted 500-fold in calf serum prior to loading.

Delivery of sample/reagents from prefilled reservoirs of the main array is accomplished by removing the insert top. The reagents flow downstream to fill the detection channel. Prefilled wash buffers from wash reservoirs flush the detection channel when the wash module lever is adjusted to 25° tilt angle.

Individual assay steps are: (1) Release sample from its reservoir to fill the detection channel and incubate for 20 min (Fig. 2A) in horizontal load position (Fig. 2B). This allows analyte proteins to be captured on Ab_1-coated sensors. (2) Move platform to wash position (25° tilt) by pushing the lever down, then release wash buffer from its reservoir (Fig. 2C). Buffer from the larger wash reservoir passes through the sample reservoir into the detection channel and flushes unbound protein to waste (Fig. 2D). (3) The platform lever is then returned to

Author Manuscript Author Manuscript Author Manuscript Author Manuscript

the load position, followed by release of Ab_2-RuBPY-SiNPs into the horizontal detection chamber, and incubation for 15 min is allowed to bind to previously captured proteins. (4) Wash unbound silica nanoparticles to waste by placing the lever in wash position. (5) TPrA solution is released from its reservoir into the horizontal detection channel, the array is placed under the CCD camera in a dark box and potential of 1.5 V vs. Ag/AgCl is applied with the supercapacitor to generate ECL for 60 s. Acquired ECL images are then processed to estimate light intensities from each microwell (Sardesai et al., 2013).

3. Results

3.1 Array Characterization & Optimization

Surface areas of the screen printed electrodes (Fig. S6, SI) were measured from cyclic voltammetry (CV) of 0.06 mM methanol (FcMeOH) in 1 M NaCl from 10 – 750 mV s^{-1} showing a diffusion-controlled, one electron reversible oxidation-reduction peak pair with separations 60–67 mV (Fig. S8A). From the slope of peak current (i_p) versus square root of scan rate ($\nu_{1/2}$) using the Randles-Sevcik equation (Bard and Faulkner, 2001), and diffusion coefficient 2.5×10^{-7} cm^2 s^{-1} (Lovelock et al., 2011) (Fig. S7, SI) estimated surface area of the printed electrodes at 0.293 ± 0.015 cm^2, RSD ± 5% (n=12). Electrochemically measured area is higher compared to geometric area of 0.071 cm^2 due to the rough, porous nature of the screen printed electrodes as confirmed by scanning electron microscopy (Fig. S6, SI). Supercapacitor was characterized by cyclic voltammetry (CV) (Fig. S8B) and by observing galvanostatic charge-discharge cycles (CC) (Fig. S8C). Results show rectangular CVs at scan rates up to 2 V s^{-1}, as well as triangular CC curves at current density 30 mA cm^{-2} suggesting nearly ideal capacitive behavior under fast charge-discharge conditions.

3.2 Reproducibility & Immunoarray Calibrations

Reproducibility of array sensors was evaluated at 0 and 500 pg mL^{-1} for the 3 protein analytes. Variation in relative ECL intensities was ≤ 7 % (n=3) array-to-array and ≤10 % spot-to-spot (n=9) (Fig. S8D&E). Out of four sensors on the array, sensors 1, 3 and 4 were used for specific protein detection. Sensor 2 at the center was used to measure background for each array, and was coated with 1 % casein only. Calibrations were done for all 3 proteins individually in calf serum, with RSD ≤ 13 % (Fig. S9, SI). Fig. S8F shows the supercapacitor mounted on a printed circuit board (PCB), connected to the array inside a dark box to generate ECL.

We tested the immunoarrays by determining several proteins simultaneously using mixtures of 3 protein standards in undiluted calf serum (Fig. 3A). Calibration curves were obtained by assigning sensor 1 to detect PSA (Fig. 3B), 2 to background, 3 to PSMA (Fig. 3C) and 4 to PF-4 (Fig. 3D). Specific capture antibodies (Ab_1) were first immobilized on the carbon sensors by adding 3 μL of Ab_1 and incubating for 2.5 hr at room temperature followed by adding 1 % casein and incubated for 1 hr. Then, protein mixtures were introduced onto these sensors, followed by the delivery of multiplexed RuBPY-SiNP ECL labels and development reagents from the prefilled chambers.

Author Manuscript Author Manuscript Author Manuscript Author Manuscript

Calibration curves for multiplexed detection were obtained by dividing average ECL signal for each concentration by control signals on each sensor chip (n=4). Dynamic ranges were from 500 fg mL^{-1} to 10 ng mL^{-1} for all protiens and detection limits as 3 times the standard deviations of zero protien controls were 300 fg mL^{-1} for PSA, 535 fg mL^{-1} for PSMA and 420 fg mL^{-1} for PF-4.

3.3 Assays of Human Serum Samples

We measured the analyte protiens from 4 prostate cancer patient serum samples and 2 cancer free human samples using the calibration curves in Fig. 5. ECL immunoassay results correlated well with single protein ELISA assays (Fig. 4. A,B&C). Linear correlation plots obtained for ELISA vs. ECL immunoarray data (Fig. S10. A,B&C, Table S1) had slopes close to 1.0 & intercepts of these plots were close to zero consistent with good correlation.

4. Discussion

Results above demonstrate successful development of inexpensive, portable, 3D-printed ECL immunoarray capable of measuring three proteins simultaneously. These arrays use light-activated supercapacitors to generate ECL. The cost per assay is ~€0.50 when the arrays are re-used with the replaceable sensor chip. The platform utilizes simple steps to complete the immunoassay in 35 min without external equipment except a CCD camera. Assay time was considered from the time serum proteins were exposed to capture antibodies till detection.

Good repeatability was found between different arrays for finite concentration with RSD ≤ ±7 % for single protein detection. RSD for various concentrations of multiplexed detection between different arrays ranged from ±1–13%, which is a little larger than desirable for bioanalytical devices. However, variability has been compromised somewhat in return for simplicity and very low cost.

Detection limits of 300 fg mL^{-1} for PSA 535 fg mL^{-1} for PSMA and 420 fg mL^{-1} for PF-4 were achieved with dynamic ranges from 500 fg mL^{-1} to 10 ng mL^{-1} (Fig. 3) that readily correspond to clinical ranges of these proteins in serum after appropriate dilutions.

Accuracy of the ECL immunoassays was confirmed by correlations to standard ELISA (Fig. 4, S10) for prostate cancer patient samples. Sample volumes as low as 5 μL were 500-fold diluted in calf serum to mimic the possibility of determining very low concentrations of proteins in a full serum matrix. These experiments revealed reasonably accurate detection of 3 analyte proteins in the presence of thousands of other proteins (Pieper et al., 2003) in mixed serum media, demonstrating high selectivity. Good correlation between ELISA and the ECL arrays with relatively small array-to-array standard deviations indicates potential for future clinical applications (Fig. 4, S10 & Table S1, SI).

These 3D-printed ECL microfluidic arrays could serve as a simple, low cost diagnostic platform for applications in both low and moderate resource environments. Printed components of the array cost ~€0.90 in materials. The screen-printed 4-sensor chip is a disposable and costs ~€0.20, whereas the reusable wash module costs ~€0.70. Considering

Author Manuscript Author Manuscript Author Manuscript Author Manuscript

all costs for immunoreagents, a single immunoassay costs ~€1.20, considering the entire platform (€0.90) to be disposable, or ~€0.50 if the wash module is reused. The 3D printed main arrays can be reused by detaching and replacing the screen printed carbon sensors. A detailed comparison of cost, time and detection limits between our ECL arrays and ELISA is provided in Table S2, SI.

Screen printing of the sensors employs an inexpensive precision desktop craft cutter for patterning templates. Using adhesive-backed patterned vinyl sheets for hand screen printing the electrodes provided acceptably reproducible sensor surface areas (±5%). Lamination after printing provides an effective hydrophobic boundary when attaching capture antibodies from aqueous solutions.

Solar panels allowed rapid light-driven charging to 1.5 V of the supercapacitor power source to drive the ECL generation step. Integration of this small power source on the immunoarray helps make it portable, avoids potentiostatic equipment, and makes the assay simpler for the operator. Future coupling of our immunosensors with a cell phone digital camera could provide a complete onsite cancer detection array for resource limited settings.

The present ECL method is general and can be adapted to other disease-related biomarkers such as proteins, nucleic acids or carbohydrates. The main requirement is that suitable pairs of antibodies or other binding agents are available for each analyte.

5. Conclusion

In conclusion, results demonstrate a novel, very low cost, gravity-flow, 3D-printed, portable immunoarray for sensitive detection of proteins. While other techniques for protein detection are competitive in terms of sensitivity, efficiency and detection limits, the novelty here is the very low cost of the system due to fabrication by 3D printing and utilization of a tiny, inexpensive, rechargeable power supply. The system results in ECL-based assays for 3 proteins that cost ~€0.50 each and can be completed in 35 min. without high level technical expertise. Using an inexpensive, robust, portable supercapacitor (€10) for power with a solar panel (€12) for recharging, the entire immunoarray costs ~€25, not including the CCD camera. A drawback of this system, however, is that a significant number of sequential tasks must be completed by the operator to complete an immunoassay. Nevertheless, this device is suitable for low and moderate resource clinical environments. This work also suggests that 3D-printing can be used to develop more sophisticated immunoarray devices with a higher level of automation.

Supplementary Material

Refer to Web version on PubMed Central for supplementary material.

ACKNOWLEDGMENTS

This work was supported financially by grant Nos. EB016707 and EB014586 from the National Institute of Biomedical Imaging and Bioengineering (NIBIB), NIH.

Author Manuscript Author Manuscript Author Manuscript Author Manuscript

REFERENCES

Afonso SA, Uliana VC, Martucci DH, Faria CR. Talanta. 2015 In press.

Anderson KB, Lockwood SY, Martin RS, Spence DM. Anal. Chem. 2013; 85:5622–5626. [PubMed: 23687961]

Aradilla D, Gentile P, Bidan G, Ruiz V, Gómez-Romero P, Schubert TJS, Sahin H, Frackowiak E, Sadki S. Nano Energy. 2014; 9:273–281.

Au AK, Bhattacharjee N, Horowitz LF, Chang TC, Folch A. Lab Chip. 2015; 15:1934–1941. [PubMed: 25738695]

Bard, AJ.; Faulkner, LR. Electrochemical Methods. 2nd ed.. New York: Wiley; 2001. p. 241-243.

Beveridge JS, Stephens JR, Williams ME. Annu. Rev. Anal. Chem. 2011; 4:251–273.

Rusling JF, Bishop GW, Doan N, Papadimitrakopoulos F. J. Materials Chem. B. 2014; 2:12–30.

Bishop GW, Satterwhite JE, Bhakta S, Kadimisetty K, Gillette KM, Chen E, Rusling JF. Anal. Chem. 2015 Ahead of Print.

Chen C, Wang Y, Lockwood SY, Spence DM. Analyst. 2014; 139:3219–3226. [PubMed: 24660218]

Chin CD, Laksanasopin T, Cheung YK, Steinmiller D, Linder V, Parsa H, Wang J, Moore H, Rouse R, Umviligihozo G, Karita E, Mwambarangwe L, Braunstein SL, van dW, Sahabo R, Justman JE, El-Sadr W, Sia SK. Nat. Med. 2011; 17:1015–1019. [PubMed: 21804541]

Chikkaveeraih BV, Bhirde A, Malhotra R, Patel V, Gutkind JS, Rusling JF. Anal. Chem. 2009; 81:9129–9134. [PubMed: 19775154]

Chikkaveeraiah BV, Mani V, Patel V, Gutkind JS, Rusling JF. Biosens. Bioelectron. 2011; 26:4477–4483. [PubMed: 21632234]

Coskun AF, Wong J, Khodadadi D, Nagi R, Tey A, Ozcan A. Lab Chip. 2013; 13:636–640. [PubMed: 23254910]

Coskun AF, Nagi R, Sadeghi K, Phillips S, Ozcan A. Lab Chip. 2013; 13:4231–4238. [PubMed: 23995895]

Dragone V, Sans V, Rosnes MH, Kitson PJ, Cronin L. Beilstein J. Org. Chem. 2013; 9:951–959. No. 109. [PubMed: 23766811]

Erkal JL, Selimovic A, Gross BC, Lockwood SY, Walton EL, McNamara S, Martin RS, Spence DM. Lab Chip. 2014; 14:2023–2032. [PubMed: 24763966]

Femmer T, Kuehne AJC, Wessling M. Lab Chip. 2014; 14:2610–2613. [PubMed: 24828586]

Forster RJ, Bertoncello P, Keyes TE. Annu. Rev. Anal. Chem. 2009; 2:359–385.

Gross BC, Erkal JL, Lockwood SY, Chen C, Spence DM. Anal. Chem. 2014; 86:3240–3253. [PubMed: 24432804]

Ge L, Wang P, Ge S, Li N, Yu J, Yan M, Huang J. Anal. Chem. 2013; 85(8):3961–3970. [PubMed: 23472854]

Giljohann DA, Mirkin CA. Nature. 2009; 462:461–464. [PubMed: 19940916]

Hawkridge AM, Muddiman DC. Ann. Rev. Anal. Chem. 2009; 2:265–277.

Hulme SE, Shevkoplyas SS, Whitesides GM. Lab Chip. 2009; 9:79–86. [PubMed: 19209338]

Kadimisetty K, Malla S, Sardesai NP, Joshi AA, Faria RC, Lee NH, Rusling JF. Anal. Chem. 2015; 87:4472–4478. [PubMed: 25821929]

Kingsmore SF. Nat. Rev. Drug Discovery. 2006; 5:310–320. [PubMed: 16582876]

Kitson PJ, Rosnes MH, Sans V, Dragone V, Cronin L. Lab Chip. 2012; 12:3267–3271. [PubMed: 22875258]

Laksanasopin T, Guo TW, Nayak S, Sridhara AA, Xie S, Olowookere OO, Cadinu P, Meng F, Chee NH, Kim J, Chin CD, Sia SK, Munyazesa E, Mugisha V, Mugwaneza P, Nsanzimana S, Rai AJ, Castro AR, Steinmiller D, Linder V, Justman JE. Sci Transl Med. 2015; 7:273re1.

Lee W, Kwon D, Jeon S, Choi W, Jung GY. Sci Rep. 2015; 5:7717. [PubMed: 25578942]

Lilja H, Ulmert D, Vickers AJ. Nat. Rev. Cancer. 2008; 8:268–278. [PubMed: 18337732]

Lovelock KRJ, Ejigu A, Loh SF, Men S, Licence P, Walsh DA. Phys. Chem. Chem. Phys. 2011; 13:10155–10164. [PubMed: 21526252]

Author Manuscript Author Manuscript Author Manuscript Author Manuscript

Malhotra R, Papadimitrakopoulos F, Rusling JF. Langmuir. 2010; 26:15050–15056. [PubMed: 20731335]

Malhotra R, Patel V, Chikkaveeraiah BV, Munge BS, Cheong SC, Zain RB, Abraham MT, Dey DK, Gutkind JS, Rusling JF. Anal. Chem. 2012; 84:6249–6255. [PubMed: 22697359]

Martin O, Averous L. Polymer. 2001; 42:6209–6219.

McDonald JC, Chabinyc ML, Metallo SJ, Anderson JR, Stroock AD, Whitesides GM. Anal. Chem. 2002; 74:1537–1545. [PubMed: 12033242]

Miao W, Bard AJ. Anal. Chem. 2004; 76:5379–5386. [PubMed: 15362895]

Otieno BA, Krause CE, Latus A, Chikkaveeraiah BV, Faria RC, Rusling JF. Biosens. Bioelectron. 2014; 53:268–274. [PubMed: 24144557]

Pieper R, Gatlin CL, Makusky AJ, Russo PS, Schatz CR, Miller SS, Su Q, McGrath AM, Estock MA, Parmar PP, Zhao M, Huang S, Zhou J, Wang F, Esquer-Blasco R, Anderson NL, Taylor J, Steiner S. Proteomics. 2003; 3:1345. [PubMed: 12872236]

Roda A, Michelini E, Cevenini L, Calabria D, Calabretta MM, Simoni P. Anal. Chem. 2014; 86:7299–7304. [PubMed: 25017302]

Rusling JF, Kumar CV, Gutkind JS, Patel V. Analyst. 2010; 135:2496–2511. [PubMed: 20614087]

Rusling JF. Anal. Chem. 2013; 85:5304–5310. [PubMed: 23635325]

Sardesai NP, Kadimisetty K, Faria R, Rusling JF. Anal. Bioanal. Chem. 2013; 405:3831–3838. [PubMed: 23307128]

Sardesai N, Pan S, Rusling JF. Chem. Commun. 2009; 33:4968–4970.

Shallan AI, Smejkal P, Corban M, Guijt RM, Breadmore MC. Anal. Chem. 2014; 86:3124–3130. [PubMed: 24512498]

Simon P, Gogotsi Y, Dunn B. Science. 2014; 343(6176):1210–1211. [PubMed: 24626920]

Siegel R, Ma J, Zou Z, Jemal A. CA Cancer. J. Clin. 2014; 64:9–29. [PubMed: 24399786]

Su C, Hsia S, Sun Y. Anal. Chim. Acta. 2014; 838:58–63. [PubMed: 25064244]

Sudarsan AP, Ugaz VM. Lab Chip. 2006; 6:74–82. [PubMed: 16372072]

Symes MD, Kitson PJ, Yan J, Richmond CJ, Cooper GJT, Bowman RW, Vilbrandt T, Cronin L. Nat. Chem. 2012; 4:349–354. [PubMed: 22522253]

Telesca D, Etzioni R, Gulati R. Biometrics. 2008; 64:10–19. [PubMed: 17501937]

Urbanski JP, Thies W, Rhodes C, Amarasinghe S, Thorsen T. Lab Chip. 2006; 6:96–104. [PubMed: 16372075]

Wang G, Zhang L, Zhang J. Chemical Society Reviews. 2012; 41(2):797–828. [PubMed: 21779609]

Wang J. Biosens. Bioelectron. 2006; 21:1887–1892. [PubMed: 16330202]

Wang Y, Liu H, Wang P, Yu J, Ge S, Yan M. Sensors and Actuators B: Chemical. 2015; 208:546–553.

Weibel DB, Kruithof M, Potenta S, Sia SK, Lee A, Whitesides GM. Anal. Chem. 2005; 77:4726–4733. [PubMed: 16053282]

Wei Q, Nagi R, Sadeghi K, Feng S, Yan E, Ki SJ, Caire R, Tseng D, Ozcan A. ACS Nano. 2014; 8:1121–1129. [PubMed: 24437470]

Wei Q, Luo W, Chiang S, Kappel T, Mejia C, Tseng D, Chan RYL, Yan E, Qi H, Shabbir F, Ozkan H, Feng S, Ozcan A. ACS Nano. 2014; 8:12725–12733. [PubMed: 25494442]

Wulfkuhle JD, Liotta LA, Petricoin EF. Nat. Rev. Cancer. 2003; 3:267–275. [PubMed: 12671665]

Yager P, Edwards T, Fu E, Helton K, Nelson K, Tam MR, Weigl BH. Nature. 2006; 442:412–418. [PubMed: 16871209]

Author Manuscript Author Manuscript Author Manuscript Author Manuscript

Highlights

- The first low cost 3D-printed immunoarray for detection of up to 3 proteins is described
- Total materials cost of the array is €1.20, and assay cost is €0.50 when the array is reused
- This is the first report of a protein biosensor powered by a supercapacitor, which is rapidly recharged using an inexpensive solar cell
- Detection of 3 proteins in serum was achieved with detection limits of 300–500 fg mL^{-1}.
- Good correlations with single-protein ELISA for 3 proteins in prostate cancer patient serum were obtained.

Author Manuscript Author Manuscript Author Manuscript Author Manuscript

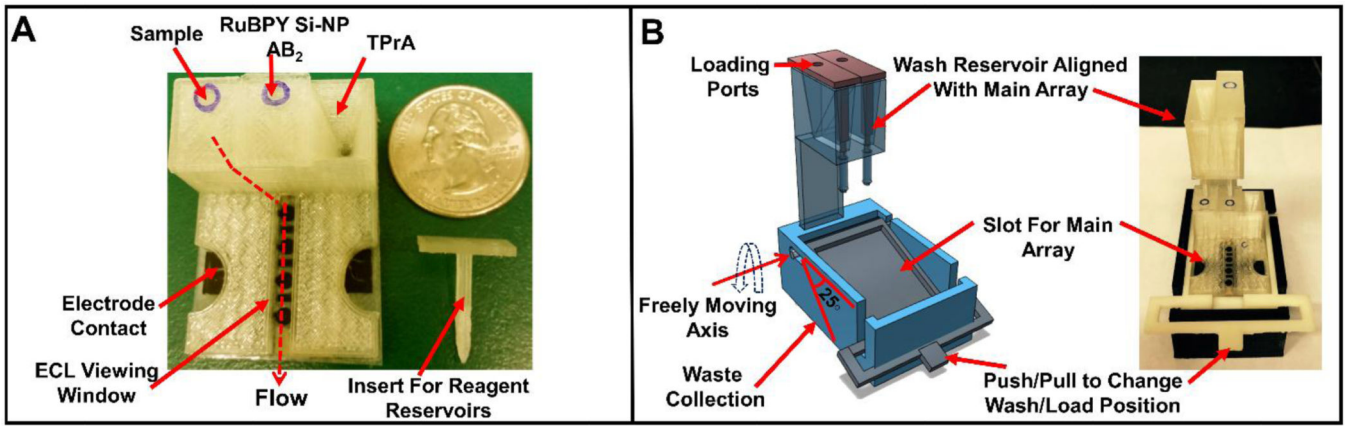

Fig. 1.

3D-printed main array and wash reservoir module. (A) Basic array showing three reagent reservoirs equipped with inserts along with flow path for reagents to reach microfluidic channel. (B) Wash reservoir module (1B Left) 3D model showing freely moving lever to change between wash and load position along with wash reservoirs aligned with main array, (1B Right) assembled immunoarray setup with both main array and wash module.

Author Manuscript Author Manuscript Author Manuscript Author Manuscript

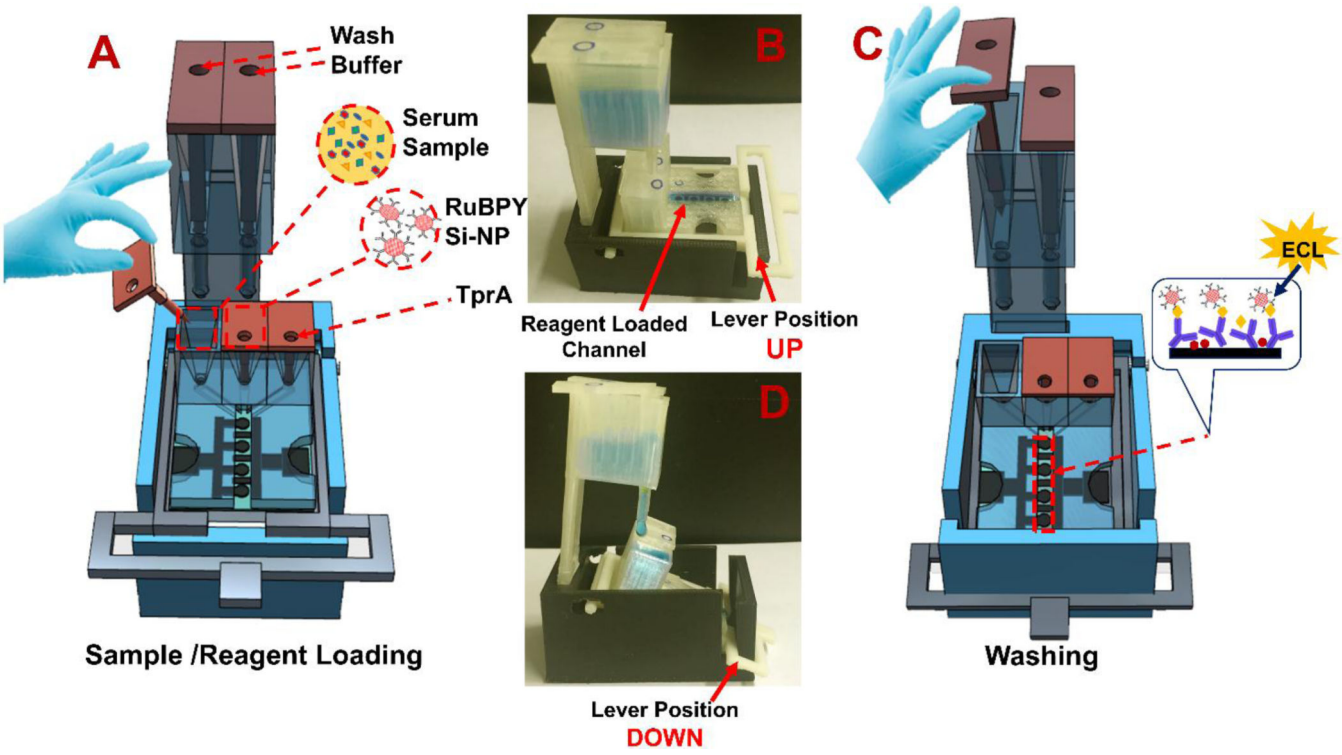

Fig. 2.

Details of the assay procedure: (A) Cartoon showing removal of insert for sample delivery from reservoir by gravity flow. (B) Load position shown with blue food color solution filling the horizontal detection channel with lever up. (C) Cartoon showing buffer delivery from wash reservoir to detection channel for washing away unbound proteins (inset shows sandwich immunoassay on sensors). (D) Wash position showing blue food color solution delivered from wash reservoir to main array when lever is down for 25° tilt of detection channel.

Author Manuscript Author Manuscript Author Manuscript Author Manuscript

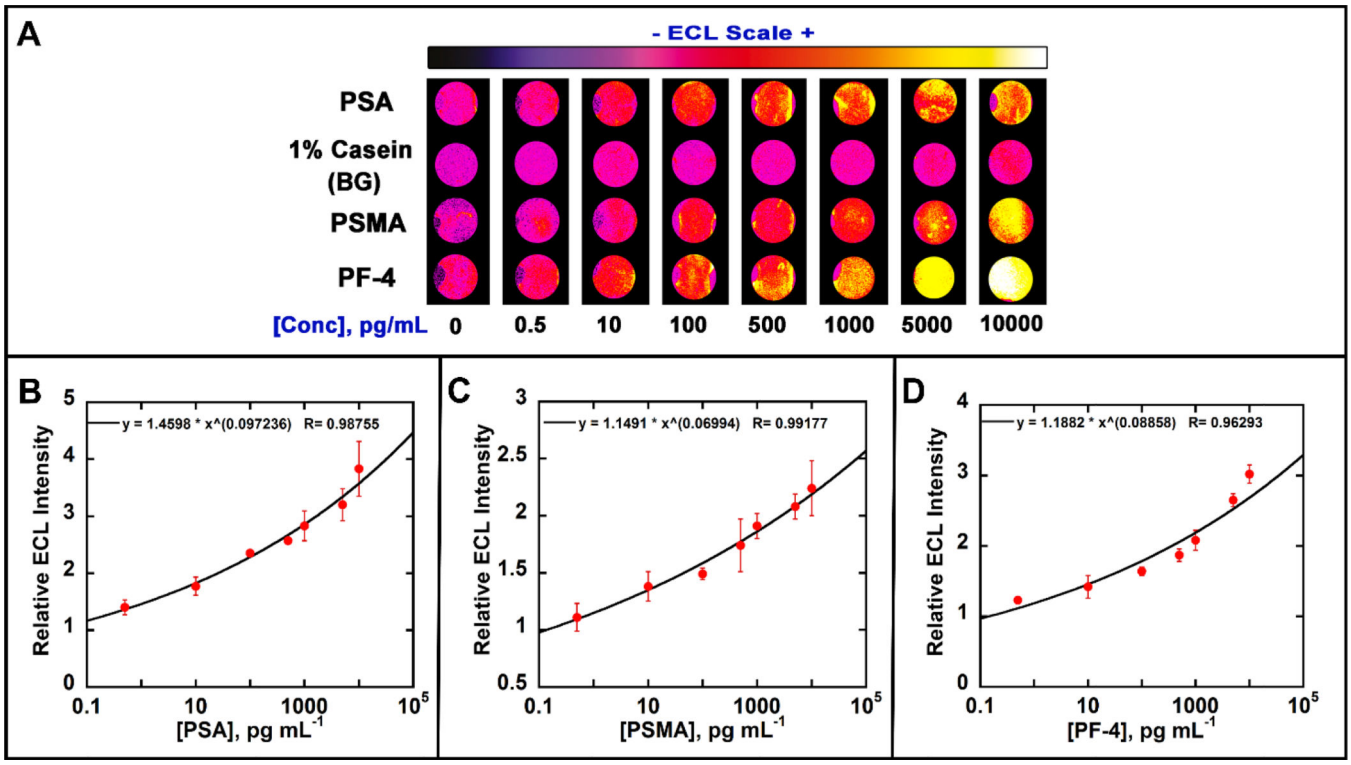

Fig. 3.

Calibration data in undiluted calf serum showing influence of biomarker protein concentration on ECL response: (A) Recolorized ECL images of 8 arrays with showing increase in ECL intensity with increased concentration. ECL signals digitized for (B) PSA, (C) PSMA and (D) PF-4 in calf serum. Error bars show standard deviation for n = 4.

Author Manuscript Author Manuscript Author Manuscript Author Manuscript

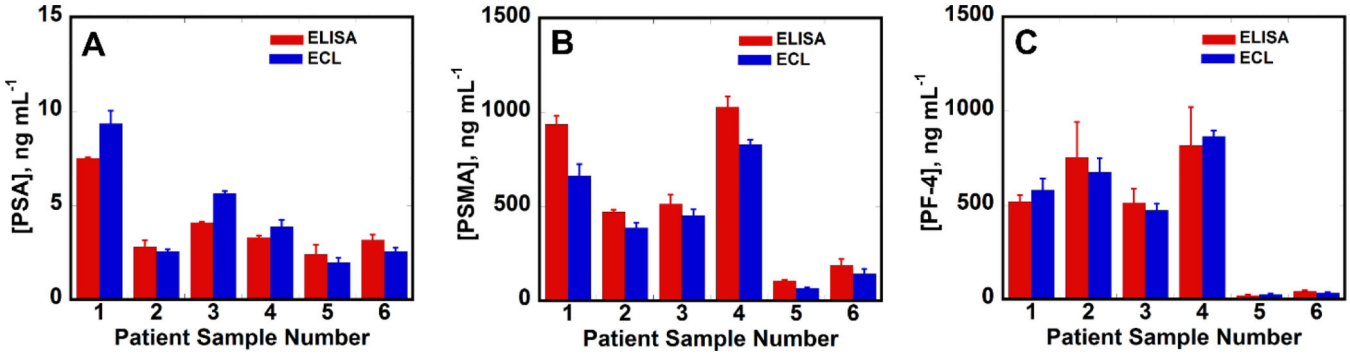

Fig. 4.

Comparisons of ECL vs. ELISA assays on human serum samples. Samples 1–4 are from prostate cancer patients and 5–6 are from cancer free individuals: (A) PSA (B) PSMA (C) PF-4 as bar graphs. Error bars are standard deviations with n=4 for ECL arrays and n=3 for ELISA.